IJRAR.ORG E-ISSN: 2348-1269, P-ISSN: 2349-5138

INTERNATIONAL JOURNAL OF RESEARCH AND ANALYTICAL REVIEWS (IJRAR) | IJRAR.ORG

An International Open Access, Peer-reviewed, Refereed Journal

Calcined Hydrotalcite materials as Efficient Adsorbents for CO_2 and N_2O Gasses

Shanigaram Prakash[1], Annumandla Ramesh[1], Erugu Bhoomika[1], Veldurthi Shashikala[1,2*]

1 – Department of chemistry, University College for Women, Osmania University, Hyderabad, Telangana, India

2 – Department of chemistry, Veeranari Chakali Ilamma Womens University, Hyderabad, Telangana, India

Abstract:

Present day major global crisis is global warming, which showed its very adverse affects on the earth, atmosphere, and mankind and on all other living organisms. CO_2 and N_2O gasses are the major components which cause global warming. N_2O is also an Ozone depleting gas. Governments of various countries are bringing different policies to control these gasses and bring awareness to the people on this issue. Scientific community has working a lot to mitigate the crisis by developing various method and materials. Different Hydrotalcites materials were studied by various authors. However there were found separate method and materials for adsorbing CO_2, converting CO_2 and decompose N_2O gasses. Present study focused on development of single material as best material for adsorbing both CO_2 and N_2O gasses. A series of four calcined hydrotalcite materials 1HT, 2HT, 3HT and 5HT were prepared with different mole ratios of Al_2O_3:MgO with 1:1, 1:2, 1:3 and 1:5 respectively. Their physical properties were studie with the help of XRD, BET – SA, SEM and TEM, their thermal stability was tested using TG-DTA and their CO_2 and N_2O adsorption properties were studied with the help of temperature programmed desorption method.

Key words: Global warming, CO_2, N_2O, Calcined Hydrotalcite, Adsorption

1. Introduction:

Climate change is a global crisis that has gained increasing attention and concern in recent years. The current state of our planet is in endanger with rising global temperatures, melting polar ice caps, more frequent extreme weather events, and shifting climate patterns [1, 2]. The Intergovernmental Panel on Climate Change (IPCC) reported that global temperatures have risen by about 1˚C above pre-industrial levels in 2017, and is expected to increase at a rate of 0.2˚C every decade [2,3]. Another important cause for the global warm is the stratospheric Ozone depletion [4] Nitrous oxide, N_2O, is one of the most harmful gases in our environment because of its contribution to the depletion of the stratospheric ozone layer and high global warming potential. N_2O catalytic decomposition represents the solution for the reduction of N_2O emissions from chemical

industry. The finding of catalyst with sufficient activity and stability in real off-gas conditions is still a problem and requires research effort in this field.

CO_2, primarily released through the combustion of fossil fuels, deforestation, and various industrial processes, acts as a potent greenhouse gas by trapping heat and intensifying the natural greenhouse effect. Anthropogenic sources of CO_2 emissions, predominantly stemming from energy production, transportation, and industrial activities, accelerated the pace of global warming and led to oceans acidification, putting tremendous stress on biodiversity. As a result, countries have pledged the Paris Agreement to limit the rise in global temperature to 1.5 ◦C above pre-industrial levels [19]. Therefore to mitigate the impact of CO_2 emissions on our climate, efficient CO_2 capture technologies need to be developed with an ambitious goal of net zero emissions by 2050 [20], so as to limit the impact of global warming [21].

Scientists have published many papers on the emission control of N2O, which has been known as one of the major greenhouse gases. N2O is an important component of the earth's atmosphere with about 150 years of life time in atmospheric condition, and has a global warming potential that is 310 times higher than that of CO2 on a per molecule basis [1–3]. In addition to the global warming effect, it acts as the main source of stratospheric NOx, which is expected to play an important role as an ozone sink when atmospheric levels of CFCs decrease. Nowadays, the global concentration of N2O is reported to be increasing faster than at any time in the past, and this has been attributed to anthropogenic contributions. The reduction of N2O emission into the atmosphere is environmentally very important, and the catalytic decomposition of N2O is an energy-efficient and promising process to attain this objective.

A variety of catalysts have been tested by many authors for the decomposition of N2O with supported or unsupported noble metals, metal-exchanged zeolites and mixed metal oxides derived from hydrotalcites. Some catalysts, such as Cu-ZSM-5 and Rh-ZSM-5 reported by Li and Armor [22], and Rh supported on ZnO reported by Oi et al. [23], were found to have prominent activities among the catalysts screened so far. Temperature programmed desorption studies of CO2 were studied to know the surface basicity as well to study the CO2 reaction on the surface of the material [24,25]. As reviewed by Kapteijn et al. [26], active catalytic systems include supported metals and oxides, mixed oxides, and zeolites. Recently, mixed oxides derived from hydrotalcite-like compounds, named ex-HTlcs, have shown high activities for N2O decomposition [5–22].

In view of wide applications of hydrotalcite materials, present work has focused on the study of hydrotalcite materials as CO2 adsorbent and N2O decomposition material. A series of four adsorbents were prepared with varing Al2O3:MgO mole ratio. And studied their temperature programmed desorption properties of CO2 and N2O gasses.

2. Experimental:

2.1. Preparation Method:

A series of four adsorbents with mole ratios of magnesium oxide to alumina with 1 : 1 (1HT), 1 : 2 (2HT), 1 : 3 (3HT) and 1 : 5 (5HT) were synthesizes by standard co-precipitation method under super saturation conditions [27]. Metal Nitrates of these oxides were taken as precursors. Corresponding weights of magnesium nitrate and aluminium nitrate salts were dissolved distilled water to make 10% solution. This salt mixture was thoroughly stirred with a mechanical stirrer to prepare a homogenous solution. Ten percent each of sodium hydroxide and sodium carbonate solutions, hydroxide and carbonate are the common interlayer anionic species, were taken in two different separating flasks and added these solutions simultaneously. Very slow and continuous addition with stirring was done, at pH 9 a thick viscous precipitate was formed stirring and addition of the precipitating agents was continued until the pH reaches to 11. Addition of these precipitating agents was performed at room temperature and after completion of the addition the temperature of the precipitant was increased to 333-338 K was kept for aging in hydrothermal conditions for 18 hrs. This gel lie precipitant was then cooled to room temperature followed by filtration. Thus obtained white cake was washed with distilled water till the filtrate shows pH of 7. Then this cake was oven dried at 393 K for overnight and calcined at 723 K for 18 h.

The Phase identification and conformation of as prepared support materials was done with the help of Rigaku XRD 6000 diffractometer with Ni filtered Cu*K*α radiation at 40 kV, 30 mA was used for X-ray diffraction analysis. N_2-physisorption analysis was carried out on a Micromeritics ASAP 2020 at 196 °C. The specific surface areas and pore size distributions of the dried and calcined hydrotalcites samples were obtained using the BET and BJH equations, respectively. The thermogravimetric analysis (TGA) experiment was performed on a SDT Q 600 TGA analyzer (TA instrument). About 10-mg sample was heated from room temperature to 973 K under oxygen atmosphere at a heating rate of 10 K/min. Formation of crystallites, their sizes, changes in morphology and layer like structure formation with increase in the percentage of magnesium oxide was studied with the help of Electron microscopic analysis that is Scanning Electron Microscopy (Hitachi S-4100 FE-SEM instrument operated at an accelerated voltage 10 kV) and Transmission electron microscopic technique on Analytical Transmission Electron Microscope (model – CM30 TEM, Philips) with an accelerating voltage 200 kV. Carbon dioxide chemisorption tests were carried out at 60°C using AutoChem 2950 Micromeritics equipment. To know the surface acidity and basicity of the calcined hydrotalcite materials CO_2 (for basicity) and NH_3 (for acidity) were studied following temperature programmed desorption studies of these gases. Quantification and strength of these acidic and basic sites were studied with the help of GC with TCD detector. A 150 mg catalyst sample was loaded in a reactor and pretreated by pure helium for 1 hour at 200°C. Then the sample was cooled to 60°C in a helium flow. The adsorption of carbon monoxide was carried by pulse chemisorption method using 10% CO_2/He mixed gas. After complete saturation the CO_2-temperature programmed desorption (CO_2-TPD) analysis performed on the same instrument. Prior to TPD experiments the sample was purged for 1h at 60°C with Helium gas and raised the reactor temperature to 850

°C at a ramp rate at 10 °C min^{-1}. The same procedure was followed for N_2O - temperature programmed desorption (N_2O-TPD) analysis.

3. Results and Discussion:

3.1. X – Ray diffraction analysis:

X – Ray diffraction analysis of as synthesized dried and calcined Mg-Al hydrotalcites with various Al_2O_3:MgO mole ratios were studied, and the diffraction patterns with characteristic peaks indicative of their crystal structure. These peaks arise from the constructive interference of X-rays diffracted by the planes of atoms present at specific 2θ angles were presented in figure 1 and figure 2 respectively. The XRD patterns of the dried samples match with the ICDD file number 890460 with sharp and symmetric peaks for (003), (006), (110), and (113) planes at 2 theta scale 11.65, 23.42, 60.95 and 62.46 respectively as well as broad symmetric peaks for the (009), (015), and (018) planes at 2 theta scale of 34.90, 39.85 and 47.59 respectively. These peaks are characteristics of clay minerals having layered structures [28, 29], and they show that in all cases, well- crystallized hydrotalcites are formed. Another important to be observed from the figure 1 i.e. XRD of LDH materials is, a perfect LDH crystal structure was present with 2HT and 3HT where the Al_2O_3:MgO mole ratio is 1:2 and 1:3 respectively. In 1HT two different materials were formed i) disordered hydrotalcite and ⟨ - aluminium hydroxide i.e. gibbsite phase with ICDD file number 77-0114 (2 theta scale and the planes are same as given above for 2HT and 3HT) and 05-0712 (2 theta scale and the planes18.74 (001), 20.3 (110) and 40.48 (201) [28, 29& 30]. And as we further increase the MgO mole ratio i.e with Al_2O_3:MgO mole ratio 1:5 there observed broadzening of the symmetric sharp peaks of LDH. This suggests that increase in the quantity of MgO either disordered layer double hydroxide is formed or small crystallites were formed. In other words increase in the MgO quantity i.e. with Al_2O_3:MgO mole ratio of 1:5 smaller crystallites of LDH were formed[27] . On calcinations of all these materials at 450 °C for 12 hrs with rate of heating 10 degrees/minut metal oxides of LDH have been separated. These two metal oxides were clearly seen in 1HT, i.e. MgO (ICDD – 87-0651) with planes 36.42 (111), 43.64 (200), 61.76 (220), 73.66 (311), 78.78 (222) and ©-alumina (ICDD 04-0875) was formed from gibbsite, corresponding to the d-spacing of the 37.44 (311), 46.03 (400), 66.76 (440) planes, and can be compared to the ICDD database (04-0875) for identification. From 1Ht to 5HT as the mole ratio of Al_2O_3:MgO increases, there was an increase in the intensities of MgO peaks and decrease in the intensities of Al_2O_3.

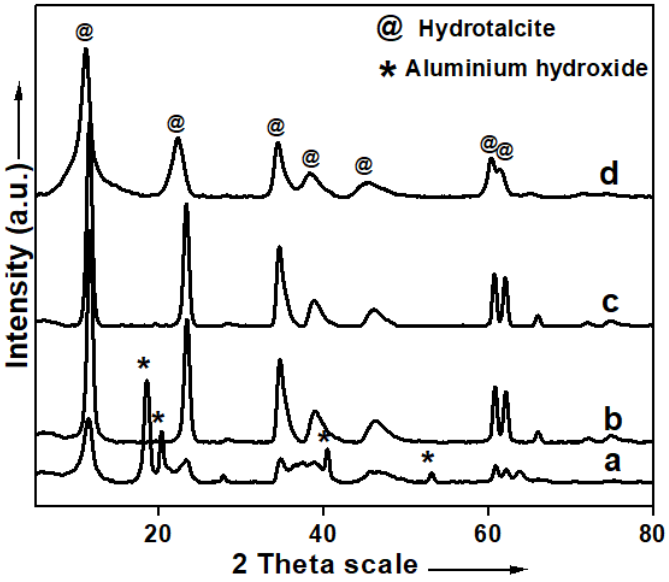

Figure 1: X – ray diffraction patterns of dried HT adsorbents a) 1HT – D b) 2HT – D, c) 3HT – D and d) 5HT – D

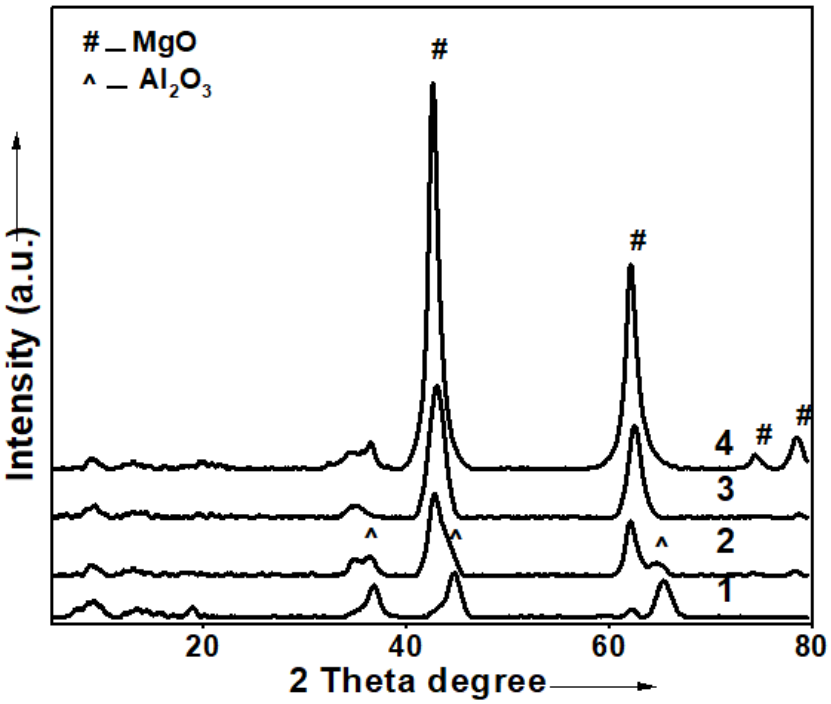

Figure 2: X – ray diffraction patterns of calcined HT adsorbents a) 1HT b) 2HT, c) 3HT and d) 5HT

3.2. BET Surface Area:

Surface areas of dried and calcined samples were obtained with the help of Brunauer–Emmett–Teller (BET) method. It explains the physical adsorption of gas molecules on solid surface and serves as the basis for an important analysis technique for the measurement of the specific surface area of materials [31]. In all the four samples there observed increase in surface area for calcined one compared to the dried samples. This may be due to presence of water molecules within the pores. There observed a general trend in the surface area of dried samples. The decreasing trend in surface area of dried samples from 1HT to 5HT can be explained due

to increase in the mole percentage of magnesia. From XRD analysis it has been found that 1HT is with aluminium hydroxide and hydrotalcite phase and in rest other three samples though there hydrotalcite phase is present x-ray amorphous magnesium hydroxide may also be present [32]. However, a reverse trend in calcined samples with increase in mole ratio of MgO was observed. This also can be understood from the XRD patterns of calcined samples. Peak broadening of magnesium oxide indicated the smaller crystallites of MgO and Al_2O_3 are responsible for increase in surface area of samples upto 3HT. XRD of the calcined 5HT sample shows sharp peaks compare to other three samples with lower magnesium oxide, which says the increase in crystallite size of the MgO in 5HT and overlapping of these large crystallites on to the smaller gamma-alumina crystallites. These two reasons may cause for the decrease in the surface are of 5HT.

Table 1: BET specific surface areas (m^2/g) of dried and calcined hydrotalcite samples

Name	**BET-SA (m^2/g)**	
	Dried	**Calcined**
1HT	201	235
2HT	186	254
3HT	172	278
5HT	150	208

3.3. TG - DTA analysis:

Thermal analysis techniques i.e. differential thermal analysis (DTA) and thermo gravimetric analysis (TGA) are useful to assess decomposition of hydrotalcite materials. The thermo gravimetric and differential thermal analysis patterns were given in figure 3 (a) and (b) respectively. It can be seen clearly that there are two broad peaks of weight loss, first one, the lower temperature loss was from 30°C to 225°C this broad peak again consists of two shoulders. First shoulder was of physically adsorbed second shoulder was of chemically adsorbed water. The second, high temperature weight loss was observed from 300 °C to 500 °C which is attributed to the loss of inter layer anions [33]. Authors Ellina Bernard et al have studied the thermogravimetric analysis of hydrotalcites prepared with various interlayer anions. They found that mono-valent anions were eluted earlier than the divalent anions [34]. Thermal decomposition mechanism of hydrotalcite materials was studied along with mass spectroscopy. The mass spectrum of the CO_2 was observed in the temperature range from 250 °C to 450 °C [35]. From the figure 4b sharp and highest weight loss was observed with the decomposition of inter layer anions i.e. carbonate ions.

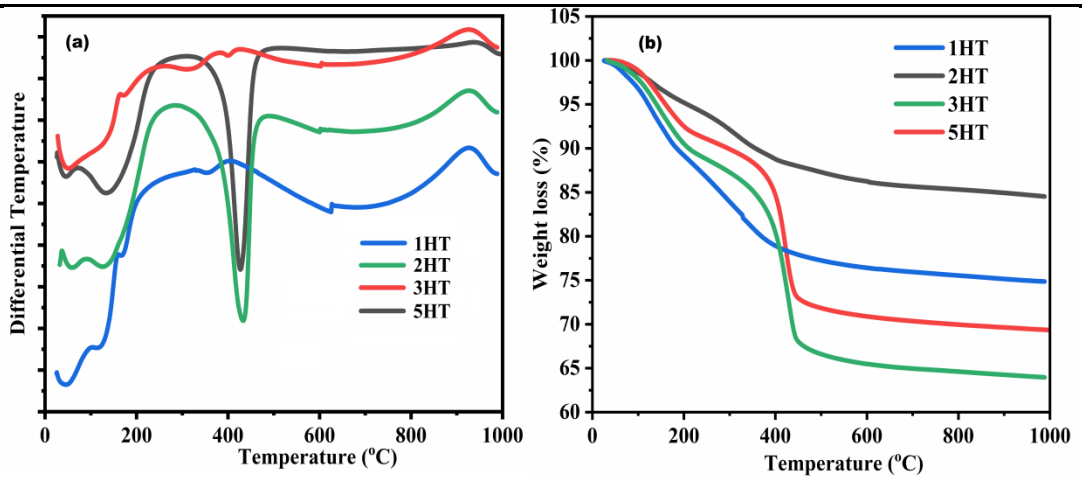

Figure 3: Comparative study of as prepared samples of 1HT, 2HT, 3HT and 5HT samples
(a) Differential thermal analysis (DTA) (b) Thermo Gravimetric Analysis (TGA)

3.4. Scanning Electron Spectroscopy (SEM):

Particles shape, size and morphology of the calcined hydrotalcite materials formed were studied with the help of scanning electron microscope and the micrographs with magnification scale 200 nm were presented in figure 4 (a), (b), (c) and (d) are of 1HT, 2HT, 3HT and 5HT respectively. Agglomerations of small crystallites were clearly seen in 1HT. Layered structure was not observed in this, XRD patterns of calcined 1HT showed small and broad peaks of alumina, peaks for magnesium oxide were not well separated, this can also be seen from the SEM image also. It can be clearly seen from micrographs (b) to (c) to (d) that as the mole ratio of MgO increases the increase in the layer structure. XRD patterns of calcined hydrotalcites of figure 1b showed increase in the intensities of MgO peaks with from 2HT to 5HT, this says that increase in the crystallite size of MgO Brucite layers. Increase in the layer structure can be observed from SEM images of 2HT, 3HT and 5HT. These layer structures are of Brucite MgO.

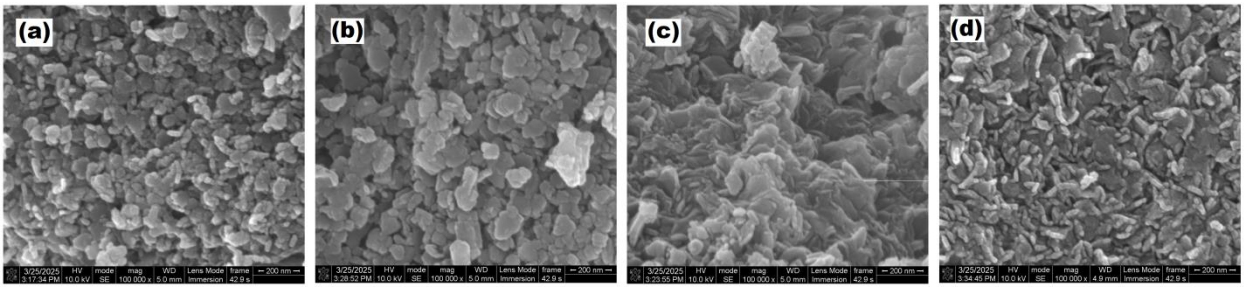

Figure 4: Scanning Electron Micrographs (scale 200 nm) of calcined (a) 1HT, (b) 2HT, (c) 3HT and (d) 5HT

3.4. Transmission Electron Spectroscopy:

To study more closely about the topography of calcined hydrotalcite materials was studied with the help of transmission electron microscopy (TEM), the micrographs with magnification scale of 30 nm were presented in the figure 5 (a), (b), (c) and (d). Very clear particles of around 15 nm width and 25 nm lengths were found in sample 1HT. From the dried samples XRD analysis (figure 1a) it was found that in this sample hydrotalcite phase was not formed completely and aluminium hydroxide phase was also seen. These are of Al_2O_3 and MgO phases in calcined 1HT. The same is conformed from the TEM image. Close observation of

TEM images of 2HT, 3HT and 5HT reveal the decrease in the number of particle like structures which are of Al_2O_3. However layer structure is increasing with increase in the mole ratio of MgO. This layer structure was of Brucite layer.

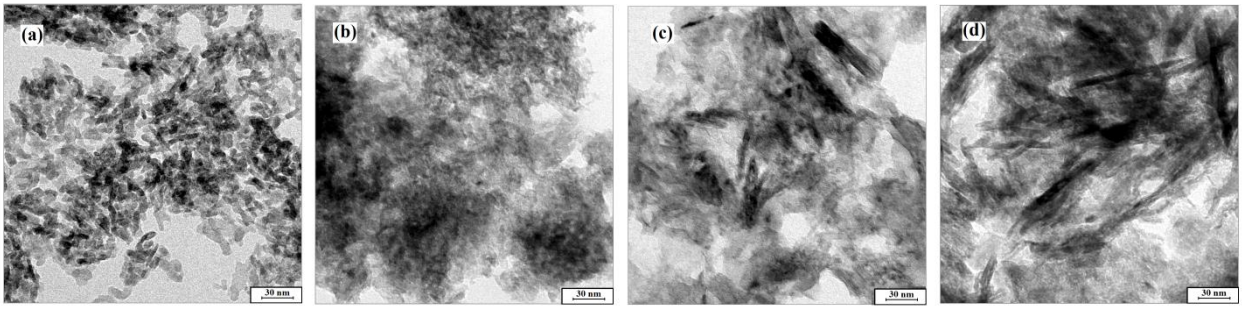

Figure 5: Transmission Electron Micrographs of calcined a) 1HT, b) 2HT, c) 3HT and d) 5HT

3.4. CO_2 Temperature Programmed Desorption:

Carbon dioxide holding capacity of the calcined hydrotalcite materials with increase in the MgO mole ratio was studied with the help of temperature programmed desorption technique. In this experiment after the adsorption of 10% CO_2/He gas, the adsorbed CO_2 was desorbed with increase in temperature in a controlled program. Thus obtained desorption curves from 1HT, 2HT, 3HT and 5HT were presented in figure 6. All these samples gave low temperature desorption peaks. 1HT gave a very less intense peak from 90 °C to 140°C, says very less amount of CO_2 was adsorbed on this material. And the desorption peak in 2HT starts from 90 °C to 223°C with a maximum at 121 °C. Desorption curve of 3HT was from 40 °C to 170 °C with peak maximum at 121 °C and a small shoulder at 80 °C. Sample 5HT shows a single desorption peak from 100 °C to 200°C with peak maximum at 126 °C. Amount of desorbed CO_2 was given in table 2. And the very low amount of desorbed CO_2 was observed for 1HT compare to other three samples. Though 1HT has equal mole ratio of Al_2O_3 : MgO from XRD analysis it was clearly seen that 1HT has more alumina phase with less MgO, SEM images also show the particulates of alumina. As the CO_2 desorption studies gives information about the types and densities of basic sites present on the surface of the materials. V.K. Díez et al have studied the CO_2 TPD in association with IR technique of magnesia alumina spinel [36]. They stated that MgO, Al_2O_3, and all the Mg*y*AlO*x* samples involves surface hydroxyl groups that can be considered as weak base sites on Mg-rich samples [37]. Single desorption peaks at low temperature might be due to the adsorption of CO_2 on the surface hydroxyl group of calcined hydrotalcite materials. Karthikeyan K. Ramasamy et al [38] have studied CO_2 adsorption on hydrotalcites calcined at various temperature and they found that there are two types of basic sites are present. According to Jianyi Shen et al. hydrotalcites calcined above 400 °C there observed transition in the Al (octahedral) –O – Mg to Al (tetrahedral) –O – Mg thus the materials calcined around 400 °C showed different CO_2 adsorption [24]. This might be the reason that whatever the mole ratio of the hydrotalcite samles, as they were calcined at 450 °C all have showed a single CO_2 adsorption maxima.

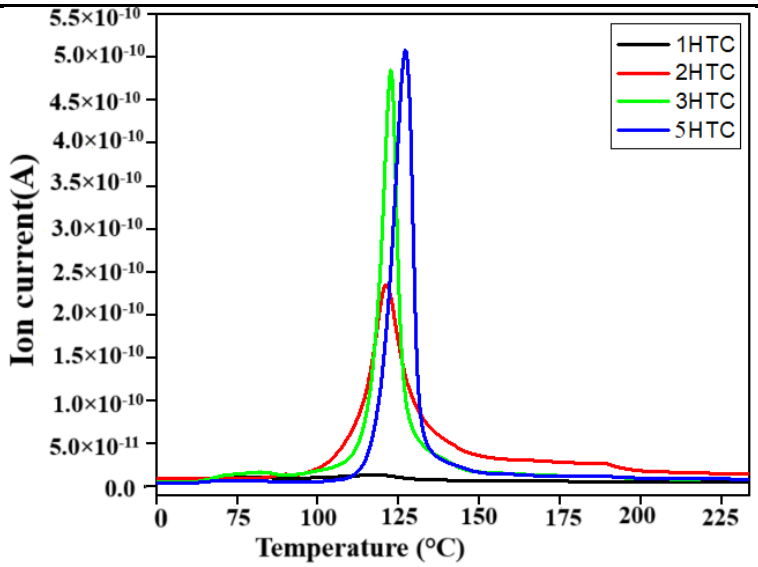

Figure 6: CO_2 Temperature programmed desorption curves of 1HT, 2HT, 3HT and 5HT

Table 2: Amount of CO_2 desorbed from calcined hydrotalcite materials

S. No.	Sample	Desorbed CO_2 (µmol/g catalyst)
1	1HT	3
2	2HT	37
3	3HT	39
4	5HT	37

3.5. N_2O Temperature Programmed Desorption:

Temperature programmed desorption (TPD) of N_2O is a technique used to study the interaction of nitrous oxide (N_2O) with surfaces, particularly its decomposition and adsorption behavior. All the calcined hydrotalcite materials were subjected to N_2O adsorption followed by temperature programmed desorption studies with increasing temperature. M.C. Román-Mart´ınez et al have studied the interaction of N_2O with a hydrotalcite-derived multimetallic mixed oxide catalyst. They studies the desorption pattern (decomposition patterns) at various temperatures starting from room temperature to 325 °C. They reported that that the amount of adsorbed gas at room temperature is large compare to higher temperatures. And found that there was not a direct relationship between adsorbed amount and reaction rate [39]. In our study it was observed that all the adsorbent HT samples show desorption peaks in the region from 100 °C to 160 °C. There observed two to four peaks merged. 1HT sowed two peaks 2HT gave three peaks 3HT and 5HT showed four peaks. This concludes that with increase in basicity the interaction of N2O with calcined hydrotalcite materials is different.

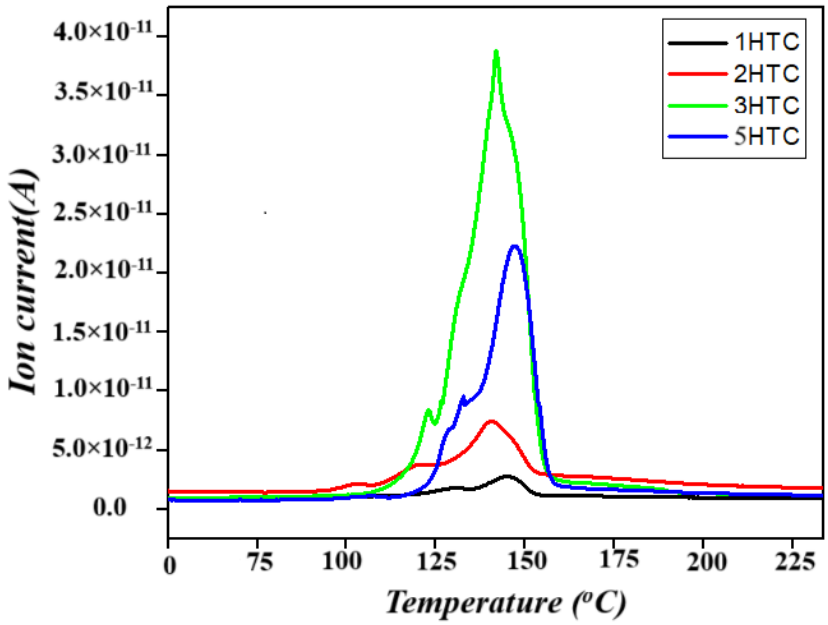

Figure 7: N_2O Temperature programmed desorption curves of 1HT, 2HT, 3HT and 5HT

Conclusion:

Crystallite phase formed before and after calcinations were studied using XRD analysis which, revealed the formation of hydrotalcite phase in every composition before the calcinations. However, 1HT showed both aluminium hydroxide and hydrotalcite phases. XRD images after calcinations showing the presence of metal oxides of Al and Mg. Except 3HT, all samples showed both Al_2O_3 and MgO phases. As the percentage of MgO increases there is sharp increase in the MgO phase. And in 3HT only one phase has MgO was observed. Thermal stabilities of these materials were compared using TG-DTA analysis. High weight loss was observed for 3HT. From micrographs of SEM and TEM it was clearly seen the increase in layer structure with increase in MgO ratio. Adsorption capacities of calcined hydrotalcites for CO_2 and N_2O gasses were studied with the help of temperature programmed desorption studies. Samples 2HT, 3HT and 5HT adsorbed good amount of CO_2. Interesting results were obtained from the N_2O temperature programmed desorption studies. From 1HT to 3HTthere observed increased N_2O adsorption properties and decreased on 5HT sample. This might be due to presence of high specific surface area and large amount of basic sites with different basic sites. Among all 3HT sample showed best activity for the CO_2 and N_2O adsorptions.

References:

1. Soo, X. Y. D., Lee, J. J. C., Wu, W., Tao, L., Wang, C., Zhu, Q., & Bu, J. (2024). Advancements in CO2 capture by absorption and adsorption: A comprehensive review. *Journal of CO2 Utilization*, *81*, 102727. https://doi.org/10.1016/j.jcou.2024.102727.

2. K.O. Yoro, M.O. Daramola, in: Advances in Carbon Capture, Woodhead Publishing, 2020, pp. 3–28.

3.Intergovernmental Panel on Climate Change(IPCC) or Edenhofer, O., & Seyboth, K. (2013b). Intergovernmental Panel on Climate Change (IPCC). In *Elsevier eBooks* (pp. 48–56). https://doi.org/10.1016/b978-0-12-375067-9.00128-5.

4.Hu, Z; Lee, J. W.; Chandran, K; Kim, S; Khanal, S. K. Nitrous oxide (N2O) emission from aquaculture: a review. Environ. Sci. Technol. 2012, 46, 6470−6470 https://doi.org/10.1021/es300110x .

5.Png, Z. M., Soo, X. Y. D., Chua, M. H., Ong, P. J., Xu, J., & Zhu, Q. (2022). Triazine derivatives as organic phase change materials with inherently low flammability. *Journal of Materials Chemistry A*, *10*(7), 3633-3641. https://doi.org/10.1039/D1TA07422A.

6. Soo, X. Y. D., Png, Z. M., Wang, X., Chua, M. H., Ong, P. J., Wang, S., ... & Zhu, Q. (2022). Rapid UV-curable form-stable polyethylene-glycol-based phase change material. *ACS Applied Polymer Materials*, *4*(4), 2747-2756. https://doi.org/10.1021/acsapm.2c00059.

7. Lee, J. J. C., Sugiarto, S., Ong, P. J., Soo, X. Y. D., Ni, X., Luo, P., ... & Zhu, Q. (2022). Lignin-g-polycaprolactone as a form-stable phase change material for thermal energy storage application. *Journal of Energy Storage*, *56*, 106118. https://doi.org/10.1016/j.est.2022.106118.

8.J.J.C. Lee, N.J.X. Lim, P. Wang, H. Liu, S. Wang, C.-L.K. Lee, D. Kai, F. Wei, R. Ji, B.H. Tan World Sci. Annu. Rev. Funct. Mater., 1 (2023), p. 2230007.

9. Soo, X. Y., Muiruri, J. K., Yeo, J. C., Png, Z. M., Sng, A., Xie, H., ... & Zhu, Q. (2023). Polyethylene glycol/polylactic acid block co-polymers as solid–solid phase change materials. *SmartMat*, *4*(3), e1188. https://doi.org/10.1002/smm2.1188.

10. Zhu, Q., Ong, P. J., Goh, S. H. A., Yeo, R. J., Wang, S., Liu, Z., & Loh, X. J. (2024). Recent advances in graphene-based phase change composites for thermal energy storage and management. *Nano Materials Science*, *6*(2), 115-138. https://doi.org/10.1016/j.nanoms.2023.09.003.

11.Irizarry, R. A., Hobbs, B., Collin, F., Beazer-Barclay, Y. D., Antonellis, K. J., Scherf, U., & Speed, T. P. (2003). Exploration, normalization, and summaries of high density oligonucleotide array probe level data. *Biostatistics*, *4*(2), 249-264. https://doi.org/10.1093/biostatistics/4.2.249

12. Wu, W. Y., Yeo, G. M. D., Wang, S., Liu, Z., Loh, X. J., & Zhu, Q. (2023). Recent progress in polyethylene-enhanced organic phase change composite materials for energy management. *Chemistry–An Asian Journal*, *18*(14), e202300391. https://doi.org/10.1002/asia.202300391

13. Zhu, Q., Yildirim, E., Wang, X., Kyaw, A. K. K., Tang, T., Soo, X. Y. D., ... & Xu, J. (2020). Effect of substituents in sulfoxides on the enhancement of thermoelectric properties of PEDOT: PSS: experimental and modelling evidence. *Molecular Systems Design & Engineering*, *5*(5), 976-984. https://doi.org/10.1039/D0ME00032A.

14. Yong, X., Wu, G., Shi, W., Wong, Z. M., Deng, T., Zhu, Q., ... & Yang, S. W. (2020). Theoretical search for high-performance thermoelectric donor–acceptor copolymers: the role of super-exchange couplings. *Journal of Materials Chemistry A*, *8*(41), 21852-21861. https://doi.org/10.1039/D0TA05765G.

15. Tang, T., Kyaw, A. K. K., Zhu, Q., & Xu, J. (2020). Water-dispersible conducting polyazulene and its application in thermoelectrics. *Chemical Communications*, *56*(65), 9388-9391. https://doi.org/10.1039/D0CC03840G.

16. Tan, X. Y., Dong, J. F., Jia, N., Zhang, H. X., Ji, R., Suwardi, A., ... & Yan, Q. Y. (2022). Enhanced near-room-temperature thermoelectric performance in GeTe. *Rare Metals*, *41*(9), 3027-3034. https://doi.org/10.1007/s12598-022-02036-8

17. Wang, X., Huang, X., Wong, Z. M., Suwardi, A., Zheng, Y., Wei, F., ... & Xu, J. (2022). Gallium-doped zinc oxide nanostructures for tunable transparent thermoelectric films. *ACS Applied Nano Materials*, *5*(6), 8631-8639. https://doi.org/10.1021/acsanm.2c02159

18. Johnson, J. R., ARCHINAL, B., KIRK, R., GADDIS, L., ANDERSON, J., BUSSEY, B., ... & DENEVI, B. (2010). The Importance of A Planetary Cartography Program: Status and Recommendations for NASA 2013-2023. *Planetary Science Decadal Survey White Paper. Available as http://www. lpi. usra. edu/decadal/sbag/topical_wp/JeffreyRJohnson. pdf*.

19. Hassan, A. M., & Tawfeeq, S. N. (2023). the Role of the United Nations in Mitigating Global Climate Change. *Russian Law Journal*, *11*(9S), 521-536.

20. Marzouk, O. A. (2025). Summary of the 2023 Report of TCEP (Tracking Clean Energy Progress) by the International Energy Agency (IEA), and Proposed Process for Computing a Single Aggregate Rating. In *E3S Web of Conferences* (Vol. 601, p. 00048). EDP Sciences.

https://doi.org/10.1051/e3sconf/202560100048

21. Chang, K. S., Lee, H., Park, Y., & Woo, J. (2006). Enhanced performances of N2O destruction in the presence of CO over the mixed metal oxide catalysts derived from hydrotalcite-type precursors. *Applied Catalysis a General*, *309*(1), 129–138. https://doi.org/10.1016/j.apcata.2006.05.007.

22. Li, Y., & Armor, J. N. (1992). Catalytic decomposition of nitrous oxide on metal exchanged zeolites. *Applied Catalysis B Environment and Energy*, *1*(3), L21–L29. https://doi.org/10.1016/0926-3373(92)80019-v.

23. Oi, J., Obuchi, A., Ogata, A., Bamwenda, G., Tanaka, R., Hibino, T., & Kushiyama, S. (1997). Zn, Al, Rh-mixed oxides derived from hydrotalcite-like compound and their catalytic properties for N2O decomposition. *Applied Catalysis B Environment and Energy*, *13*(3–4), 197–203. https://doi.org/10.1016/s0926-3373(96)00105-1.

24.Shen, J., Tu, M., & Hu, C. (1998). Structural and surface Acid/Base properties of Hydrotalcite-Derived MGALO oxides calcined at varying temperatures. *Journal of Solid State Chemistry*, *137*(2), 295–301. https://doi.org/10.1006/jssc.1997.7739.

25.Kumar, V. S., Nagaraja, B. M., Shashikala, V., Seetharamulu, P., Padmasri, A. H., Raju, B. D., & Rao, K. R. (2004). Role of acidic and basic sites of Al2O3 in predicting the reaction pathway of isophorone transformation. *Journal of Molecular Catalysis A: Chemical*, *223*(1-2), 283-288. https://doi.org/10.1016/j.molcata.2003.08.034.

26. Kapteijn, F., Rodriguez-Mirasol, J., & Moulijn, J. A. (1996). Heterogeneous catalytic decomposition of nitrous oxide. *Applied Catalysis B Environment and Energy*, *9*(1–4), 25–64. https://doi.org/10.1016/0926-3373(96)90072-7

27. Miyata, S. (1975). The syntheses of hydrotalcite-like compounds and their structures and physico-chemical properties—I: the systems Mg 2+-Al 3+-NO 3−, Mg 2+-Al 3+-Cl−, Mg 2+-Al 3+-ClO 4−, Ni 2+-Al 3+-Cl− and Zn 2+-Al 3+-Cl−. *Clays and Clay Minerals*, *23*, 369-375. . https://doi.org/10.1346/ccmn.1975.0230508.

28.Ke, X., Bernal, S. A., Provis, J. L., & Lothenbach, B. (2020). Thermodynamic modelling of phase evolution in alkali-activated slag cements exposed to carbon dioxide. *Cement and Concrete Research*, *136*, 106158. https://doi.org/10.1016/j.cemconres.2020.106158.

29.Park, S., Lothenbach, B., Jang, J. G., Kim, H. K., & Lee, N. (2023). Thermodynamic modeling and experimental study of carbonation of alkali-activated slag cements. *ACS Sustainable Chemistry & Engineering*, *11*(10), 4049-4063. https://doi.org/10.1021/acssuschemeng.2c05789.

30. Ramesh, T. N. (2013). Mechanism of structural transformations during thermal decomposition studies of aluminium hydroxide polymorph. *Inernational J. Sci. Res*, *1*, 514-518.

31. Brunauer, S., Emmett, P. H., & Teller, E. (1938). Adsorption of gases in multimolecular layers. *Journal of the American Chemical Society*, *60*(2), 309–319. https://doi.org/10.1021/ja01269a023.

32. Rouquerol, F., Rouquerol, J., & Sing, K. (1999). Assessment of mesoporosity. In *Elsevier eBooks* (pp. 191–217). https://doi.org/10.1016/b978-012598920-6/50008-7.

33. Pérez-Ramírez, J., & Abelló, S. (2006). Thermal decomposition of hydrotalcite-like compounds studied by a novel tapered element oscillating microbalance (TEOM). *Thermochimica Acta*, *444*(1), 75–82. https://doi.org/10.1016/j.tca.2006.02.031.

34. Bernard, E., Zucha, W. J., Lothenbach, B., & Mäder, U. (2021). Stability of hydrotalcite (Mg-Al layered double hydroxide) in presence of different anions. *Cement and Concrete Research*, *152*, 106674. https://doi.org/10.1016/j.cemconres.2021.106674.

35. Crosby, S., Tran, D., Cocke, D., Duraia, E., & Beall, G. (2014). Effect of isomorphous substitution on the thermal decomposition mechanism of hydrotalcites. *Materials*, *7*(10), 7048–7058. https://doi.org/10.3390/ma7107048.

36. Dıez, V. K., Apesteguıa, C. R., & Di Cosimo, J. I. (2003). Effect of the chemical composition on the catalytic performance of MgyAlOx catalysts for alcohol elimination reactions. *Journal of Catalysis*, *215*(2), 220-233. https://doi.org/10.1016/S0021-9517(03)00010-1.

37.T. Kanno, M. Kobayashi, in: M. Misono, Y. Ono (Eds.), Acid–Base Catalysts II, Kodansha/Elsevier, Tokyo/Amsterdam, 1994, pp. 207–211.

38. Ramasamy, K. K., Gray, M., Job, H., Santosa, D., Li, X. S., Devaraj, A., ... & Wang, Y. (2016). Role of calcination temperature on the hydrotalcite derived MgO–Al 2 O 3 in converting ethanol to butanol. *Topics in Catalysis*, *59*, 46-54.

39. Román-Martınez, M. C., Kapteijn, F., Cazorla-Amorós, D., Pérez-Ramırez, J., & Moulijn, J. A. (2002). A TEOM-MS study on the interaction of N2O with a hydrotalcite-derived multimetallic mixed oxide catalyst. *Applied Catalysis A: General*, *225*(1-2), 87-100. https://doi.org/10.1016/S0926-860X(01)00770-0.